

# Prospects in Constraining the Dark Energy Potential

Enrique Fernandez-Martinez<sup>1</sup> & Licia Verde<sup>2</sup>

<sup>1</sup>*Max Planck Institut für Physik, Föhringer Ring, 6. München, D-80805 Germany*

<sup>2</sup>*ICREA & Institute of Space Sciences (IEEC-CSIC), Fac. Ciencies, Campus UAB, Torre C5 parell 2, Bellaterra, Spain and Dept. of Astrophysical sciences, Peyton Hall, Ivy Lane, Princeton University, Princeton, NJ*

**Abstract.** We generalize to non-flat geometries the formalism of Simon et al. (2005) to reconstruct the dark energy potential. This formalism makes use of quantities similar to the Horizon-flow parameters in inflation, can, in principle, be made non-parametric and is general enough to be applied outside the simple, single scalar field quintessence. Since presently available and forthcoming data do not allow a non-parametric and exact reconstruction of the potential, we consider a general parametric description in term of Chebyshev polynomials. We then consider present and future measurements of  $H(z)$ , Baryon Acoustic Oscillations surveys and Supernovae type 1A surveys, and investigate their constraints on the dark energy potential. We find that, relaxing the flatness assumption increases the errors on the reconstructed dark energy evolution but does not open up significant degeneracies, provided that a modest prior on geometry is imposed. Direct measurements of  $H(z)$ , such as those provided by BAO surveys, are crucially important to constrain the evolution of the dark energy potential and the dark energy equation of state, especially for non-trivial deviations from the standard  $\Lambda$ CDM model.

## 1. Introduction

Recent observations e.g., [1, 2, 3, 4, 5, 6, 7] indicate that the present-day energy density of the universe is dominated by a “dark energy” component, responsible for the current accelerated expansion.

The leading dark energy candidates are a cosmological constant or a slowly varying rolling scalar field e.g., [8, 9, 10, 11, 12, 13, 14] and [15] for a review, although explanations in terms of modifications of the Friedman equation ([16, 17, 18, 19, 20, 21, 22, 23, 24, 25] and references therein, under the name of “modifications of gravity” and e.g., [26, 27, 28, 29] under the name of inhomogeneous models) are also being widely investigated.

An extended observational effort is being carried out (e.g., SNLS, SDSS, PanStarrs etc.) and ambitious plans for the future are being proposed or planned (e.g., DES, PAU, BOSS, WFMOS, SNAP, ADEPT, DUNE, SPACE, SKA, LSST) with the goal of shedding light on the nature of dark energy. With few exceptions, current constraints on the nature of dark energy measure an integrated value over time of the Hubble parameter,  $H(z)$ , which in turn is an integral of its equation of state parameter ( $w = p/\rho$ , with  $p$  denoting pressure and  $\rho$  density). While these constraints are very tightly centered around the cosmological constant value, with a 15% error, the finding that the average value of  $w$  is consistent with  $-1$  does not exclude the possibility that  $w$  varied in time e.g., [30]. An emerging technique in dark energy studies uses observations of the so-called baryon acoustic oscillations (BAO) [31, 32, 33]. The BAO yield a measurement of the sound horizon at recombination, a standard ruler visible at different epochs in the lifetime of the Universe: at the last scattering surface through cosmic microwave background observations and at lower redshifts through galaxy clustering. In galaxy surveys, the BAO scale can be measured both along and perpendicular to the line sight. In particular the line-of-sight measurement offers the unique opportunity to measure directly  $H(z)$ , rather than its integral.

To improve our understanding of dark energy, it is important not only to ask whether this dark energy component is dynamical or constant, but also, to constrain possible shapes of the dark energy potential. As different theoretical models are characterized by different potentials, a reconstruction of the dark energy potential from cosmological observations could help discriminating among different, physically motivated, models.

Different approaches to the reconstruction of the dark energy equation of state or potential have been proposed in the literature e.g., [34, 35, 36, 37]. In this paper we build upon and generalize the reconstruction technique proposed in [36] to non-flat universes. In fact [38] showed that there can be a degeneracy between geometry and dark energy properties, thus analyses to constrain dark energy parameters should be carried out varying jointly the geometry of the Universe.

We then apply this reconstruction to existing determinations of  $H(z)$  from ages of passively evolving galaxies [36], to new Supernovae data [5], and we forecast the constraints on the dark energy potential achievable with the next generation of BAO

and Supernova surveys. We find that relaxing the assumption of flatness increases the error in the reconstructed dark energy evolution but does not open up degeneracies, provided that a modest prior on geometry is imposed: a Gaussian prior on  $\Omega_k$  with *r.m.s.*  $\sigma_k = 0.03$ . Measurements of  $H(z)$  such as those provided by BAO surveys, are crucial to constrain the dark energy evolution and to break degeneracies among dark energy parameters, for non-trivial deviations from the simplest  $\Lambda$ CDM model.

The rest of the paper is organized as follows: in §2 we present our reconstruction of the dark energy potential. In §3 we describe the priors used in addition to the present and future data sets we consider. Our results on the dark energy potential reconstruction are reported in §4. For completeness, we present a similar reconstruction applied to the dark energy equation of state parameter as a function of redshift (in §5). We conclude in §6.

## 2. How to reconstruct the dark energy potential from observations

Ref. [36] presented a non-parametric method to reconstruct the redshift evolution of the potential and kinetic energy densities of the dark energy field, using quantities similar to the Horizon-flow parameters in inflation e.g., [39, 40]. As a fully non-parametric reconstruction would require the knowledge of  $H(z)$  and of  $\dot{H}(z)$ , [36] also presented a general parameterization of the dark energy potential as a function of redshift,  $V(z)$ , in term of Chebyshev polynomials and showed how to reconstruct the potential as a function of the scalar field  $V(\phi)$  from  $V(z)$ . In this section we will follow Ref. [36] to directly relate the dark energy potential  $V(\phi)$  with observable quantities, but we generalize their approach to non-flat universes.

We restrict ourselves to classical configurations  $\phi = \phi(t)$ , that do not break the homogeneity and isotropy of space-time. The energy-momentum tensor of this scalar field configuration is that of a perfect fluid, with density  $\rho_\phi$  and pressure  $p_\phi$  given by

$$\rho_\phi = K(\phi) + V(\phi), \quad p_\phi = K(\phi) - V(\phi) \quad \text{and} \quad K \equiv \frac{1}{2}\dot{\phi}^2. \quad (1)$$

where  $K$  denotes the kinetic energy of the field. The Friedmann's equations then read:

$$H^2 = \frac{\kappa}{3} (\rho_T + \rho_\phi + \rho_k), \quad (2)$$

$$\frac{\ddot{a}}{a} = \frac{1}{2H} \frac{dH^2}{dt} = -\frac{\kappa}{6} (\rho_T + 3p_T + \rho_\phi + 3p_\phi), \quad (3)$$

where  $\kappa = 8\pi/m_p^2$  (or  $\kappa = 8\pi G$ ) and  $\rho_k = -k \frac{3c^3}{\kappa a^2}$ , where  $k$  is the curvature. In Eq. (3) we introduced the compact notation  $\rho_T$  and  $p_T$  for the total energy density and pressure. Using both Friedmann's equations to solve for the kinetic energy of the field and considering a single matter component we obtain:

$$3H^2(z) - \frac{1}{2}(1+z) \frac{dH^2(z)}{dz} = \kappa \left( V(z) + \frac{1}{2}\rho_m(z) + \frac{2}{3}\rho_k(z) \right), \quad (4)$$

An exact non-parametric reconstruction of  $V(z)$  is possible only if  $H(z)$  and  $\dot{H}(z)$  are known (see Ref. [36] for details). Unfortunately present and near future prospective

data do not allow this level of precision. However if  $V(z)$  can be parameterized, Eq. (4) can be integrated analytically:

$$H^2(z) = \left( H_0^2 - \frac{\kappa}{3}(\rho_{m,0} + \rho_{k,0}) \right) (1+z)^6 + \frac{\kappa}{3}(\rho_m(z) + \rho_k(z)) - 2(1+z)^6 \int_0^z V(x) (1+x)^{-7} dx . \quad (5)$$

Hereafter the 0 subscript denotes the quantity evaluated at  $z = 0$ .

An interesting parameterization of the potential involves the Chebyshev polynomials, which form a complete set of orthonormal functions on the interval  $[-1, 1]$ . They also have the interesting property to be the minimax approximating polynomial, that is, the approximating polynomial which has the smallest maximum deviation from the true function at any given order. We can thus approximate a generic  $V(z)$  as

$$V(z) \simeq \sum_{n=0}^N \lambda_n T_n(x) \quad (6)$$

where  $T_n$  denotes the Chebyshev polynomial of order  $n$  and we have normalized the redshift interval so that  $x = 2z/z_{max} - 1$ ;  $z_{max}$  is the maximum redshift at which observations are available and thus  $x \in [-1, 1]$ . Since  $|T_n(x)| \leq 1$  for all  $n$ , for most applications, an estimate of the error introduced by this approximation is given by  $\lambda_{N+1}$ . With this parameterization, the relevant integral in Eq. (5) becomes:

$$\begin{aligned} \int_0^z V(y)(1+y)^{-7} dy &= \frac{z_{max}}{2} \sum_{n=0}^N \lambda_n \int_{-1}^{2z/z_{max}-1} T_n(x)(a+bx)^{-7} dx \\ &\equiv \frac{z_{max}}{2} \sum_{n=0}^N \lambda_n F_n(z) \end{aligned} \quad (7)$$

where  $a = 1 + z_{max}/2$  and  $b = z_{max}/2$ . These integrals can be solved analytically for any order  $n$  and  $F_n$  are known analytic functions. Substituting in (5) we finally obtain:

$$\begin{aligned} H^2(z, \lambda_i) &= (1+z)^6 H_0^2 \left[ 1 - 3z_{max} \sum_{n=0}^N \frac{\lambda_n}{\rho_c} F_n(z) \right. \\ &\quad \left. - \Omega_{m,0} \left( 1 - \frac{1}{(1+z)^3} \right) - \Omega_{k,0} \left( 1 - \frac{1}{(1+z)^4} \right) \right] , \end{aligned} \quad (8)$$

which relates observable quantities such as the Hubble parameter and  $\Omega_{m,0}$  with the coefficients of the Chebyshev expansion of the potential. Determining the coefficients  $\lambda_i$  in this manner allows one to reconstruct  $V(z)$  as in (6). To obtain  $V(\phi)$ , however, we would also need to reconstruct  $\phi(z)$ . This can also be accomplished from the determination of the coefficients  $\lambda_i$ , through the kinetic energy of the field. From the first Friedmann equation we have:

$$\begin{aligned} K(z) &= \frac{1}{2} \left( \frac{d\phi}{dz} \right)^2 (1+z)^2 H^2(\lambda_i, z) \\ &= 3\kappa^{-1} H^2(\lambda_i, z) - \rho_m(z) - \rho_k(z) - V(\lambda_i, z) , \end{aligned} \quad (9)$$

which can be integrated to obtain  $\phi(z)$  and thus  $V(\lambda_i, \phi)$  from  $V(\alpha_i, z)$ :

$$\begin{aligned} \phi(z) - \phi(0) = \\ \pm \int_0^z \frac{\sqrt{6\kappa^{-1} H^2(\lambda_i, z) - 2\rho_m(z) - 2\rho_k(z) - 2V(\lambda_i, z)}}{(1+z) H(\lambda_i, z)} dz \end{aligned} \quad (10)$$

where the ambiguity in sign comes from the quadratic expression for the kinetic energy. Typically, if we think of a scalar field rolling slowly along its potential, the plus sign will be the relevant one.

In what follows we will only consider a three parameters model (i.e.  $N = 2$ ). Even with only three parameters, if the fiducial model is a  $\Lambda$ CDM, the forecasted constraints on deviations from a flat potential are rather weak especially at  $z > 0.5$ . However, with the formulation presented here, one can pose the question of how many dark energy parameters are required by the data. Techniques such as cross validation [41, 42, 43] could be used to address the issue.

In the next sections we describe the different observables we consider to probe the dark energy potential.

### 3. Datasets and priors

Most probes of dark energy measure integrated quantities, for example Supernovae measure the luminosity distance  $d_L(z)$ . There are two known techniques to reconstruct directly  $H(z)$ . One is through the measurement of the BAO scale in the radial direction through  $dr = c/H(z)dz$ . Current surveys do not yet have the sufficient statistical power to do so and thus current measurements are angle-averaged. However, forthcoming and future surveys promise to deliver  $H(z)$  determination with % accuracy. BAO surveys, of course, also provide measurement of the angular diameter distance  $d_A(z)$ .

The other technique relies on the measurement of ages of passively evolving galaxies. It has been demonstrated by recent observations that massive ( $L > 2L_*$ ) luminous red galaxies have formed more than 95% of their stars at redshifts  $> 4$ . Since then, stars in these galaxies have been evolving passively. They are therefore, excellent cosmic clocks, where the age of their stars can be inferred from the integrated stellar spectrum using stellar evolution theory.

BAO surveys along with large samples of type 1A Supernovae are among the leading techniques to constrain dark energy and an extensive experimental effort is being carried out. For this reason we consider presently available “cosmic clocks” data, presently available Supernovae data and future BAO and Type 1A supernova surveys.

#### 3.1. Priors

In what follows we assume a flat  $\Lambda$ CDM with  $H_0 = 73.2 \text{ Km s}^{-1}\text{Mpc}^{-1}$  and  $\Omega_m = 0.24$  fiducial model. In all cases we consider Gaussian priors of  $\sigma_H = 8 \text{ Km s}^{-1}\text{Mpc}^{-1}$  for  $H_0$ ,  $\sigma_{w_m} = 0.01$  for  $\Omega_m h^2$  and  $\sigma_k = 0.03$  for  $\Omega_k$ . This is motivated by the fact that current data already constrain these parameters at this level e.g., [44, 2, 4]. We will assume here

that these parameters can be constrained at this level by combination of e.g., Cosmic Microwave Background experiments (e.g., Planck [45]) and local determinations of the Hubble parameter [46].

### 3.2. Baryon Acoustic Oscillations

Dark matter overdensities in the early Universe produce acoustic waves in the photon-baryon plasma that propagate with the speed of sound until the recombination era, when photons decouple from baryons and free stream. The baryon wave then stops propagating leaving an imprint at a characteristic distance from the original dark matter overdensity: the sound horizon length. This process thus provides a standard ruler at which the correlation function of dark matter (and thus of galaxies) should peak (e.g., [31]). Evidence of this peak has already been reported in galaxy surveys e.g., [32, 33]. Measuring this standard ruler at different redshifts would provide a powerful probe of the expansion history of the Universe and thus of the dark energy potential.

Baryon Acoustic Oscillations (BAO) can be measured both along and perpendicular to the line sight. An angular measurement of the BAO scale at redshift  $z$  would then give:

$$\Delta\theta = \frac{r_{BAO}}{(1+z)d_A(z)} , \quad (11)$$

where  $d_A(z) = 1/(1+z) \int_0^z c/H(z)dz$  and  $r_{BAO}$  is the BAO scale. This measurements of  $d_A(z)$  can then be compared to Eqs. (8) or (21, below in §5.) to derive constraints on the coefficients  $\lambda_i$  or  $w_i$  respectively. Alternatively, if the redshift precision of the survey is good enough, the BAO scale could be measured along the line of sight as

$$\Delta z = H(z)r_{BAO} , \quad (12)$$

thus providing a direct measurement of  $H(z)$ .

To forecast the errors with which  $H(z)$  and  $d_A(z)$  will be recovered we make use of the formulas derived in [47], where a grid of BAO surveys was simulated with different survey parameters and the accuracy found for the observables was fitted to the following formulas:

$$\sigma_d(z_i) = x_0^d \frac{4}{3} \sqrt{\frac{V_0}{V_i}} f_{nl}(z_i) \quad (13)$$

$$\sigma_H(z_i) = x_0^H \frac{4}{3} \sqrt{\frac{V_0}{V_i}} f_{nl}(z_i) \quad (14)$$

where

$$f_{nl}(z_i) = \begin{cases} 1 & z < z_m \\ (\frac{z_m}{z_i})^\gamma & z > z_m \end{cases} \quad (15)$$

$V_i$  is the volume of the redshift bin  $z_i$ . The fitting formula was motivated by the assumption that the accuracy achievable in the observables will be proportional to the fractional error with which the power spectrum can be recovered

$$\frac{\Delta_P}{P} \simeq \sqrt{\frac{2}{N_m}} \left( 1 + \frac{1}{nP} \right) , \quad (16)$$

where  $N_m \propto V_i$  is the number of Fourier modes contributing to the measurement and  $n$  the number density of galaxies surveyed. Non-linearities tend to erase the acoustic peaks via mode-coupling: the function in (15) takes into account that, at increasing redshift, increasingly small scales are in the linear regime. The fitting parameters were calibrated on N-body simulations by [47] and found to be:  $x_0^H = 0.0148$ ;  $x_0^d = 0.0085$ ;  $V_0 = 2.16/h^3$ ;  $z_m = 1.4$ ;  $\gamma = 0.5$ .

Here we will consider two setups that roughly encompass ground-based (“ground”) and space-based (“space”) perspective BAO surveys. The survey parameters are summarized in Table 1. In both cases we assume that shot noise is unimportant at the scale of interest and that the redshift determination is good enough to measure the radial BAO signal. Along the way we will also report the results for the angular-only BAO. This case will be relevant to photometric surveys that can achieve photometric errors better than  $\sim 4\%$  [48, 49]

Survey	Area ( $dg^2$ )	$z_{min}$	$z_{max}$	bins in $z$
ground	10000	0.1	1	9
space	30000	1	2	10

**Table 1.** Survey parameters of the two BAO surveys considered.

### 3.3. Galaxy Ages

The Hubble parameter depends on the differential age of the Universe as a function of redshift via  $H(z) = dz/dt(1+z)^{-1}$ . The feasibility of measuring  $H(z)$  from high-resolution, high signal-to-noise spectra of passively evolving galaxies was demonstrated in [50, 36, 51]. Here we use the  $H(z)$  determination obtained by [36] and publicly available at [52], from a compilation of data at  $0 < z < 1.8$  and generalize the analysis of [36] to non flat universes. Recent studies [53, 54] have clearly established that massive ( $> 2.2L_*$ ) luminous red galaxies have formed more than 95% of their stars at redshifts higher than 4. These galaxies, therefore, form a very uniform population, whose stars are evolving passively after the very first short episode of star active star formation [53, 54, 55]. Because the stars evolve passively, these massive LRG are excellent cosmic clocks, i.e. they provide a direct measurement of  $dt/dz$ ; the observational evidence discards further star formation activity in these galaxies. Dating of the stellar population can be achieved by modeling the integrated light of the stellar population using synthetic stellar population models, in a similar way to what is done for open and globular clusters in the Milky Way. The dating of the stellar population needs to be done on the integrated spectrum because individual stars are not resolved and therefore the requirements on the observed spectrum are stringent as one needs a very wide wavelength coverage, spectral resolution and very high signal-to-noise. Ref. [54] has shown that the spectra of these massive LRG at a redshift  $\sim 0.15$  are extremely similar, with differences of only 0.20 mmag, which is another evidence of the uniformity of the stellar populations in these

galaxies. There have been already examples of accurate dating of the stellar populations in LRGs ([56, 57, 50, 36]) where it has been shown that galaxy spectra with sufficient wavelength coverage (the UV region is crucial), wavelength resolution (about 3 Å) and enough S/N (at least 20 per resolution element of 3 Å) can provide sensible constraints on cosmological parameters. More details can be found in [36, 58].

### 3.4. Supernovae

The intrinsic luminosity of Type IA Supernovae (SN) can be accurately predicted from the decay rate of the Supernovae brightness. This provides bright standard candles that can be observed up to redshifts  $z > 1$ . Measuring SN apparent magnitude, the luminosity distance can thus be inferred:

$$d_L(z) = (1+z) \int_0^z \frac{c}{H(z)} dz . \quad (17)$$

If their redshift is also measured, Type IA Supernova provide information on the integral of  $1/H(z)$  and hence on the cosmological parameters. In this way Supernovae provided the first direct evidence for the accelerated expansion of the Universe [59, 60].

We consider present and forecasted Type IA Supernovae data in the analysis of Section 4. For the present Supernovae data we use the sample of [61]. For future Supernovae data we assume 1000 Supernovae distributed in 5 redshift bins between 0.8 and 1.3 plus a sample of 500 Supernovae at low redshift [62, 25]. Table 2 summarizes the distribution of the Supernovae considered.

Mean z	0.1	0.85	0.95	1.05	1.15	1.25
SN	500	231	219	200	183	167

**Table 2.** Redshift distribution of the forecasted Supernovae sample.

We consider a statistical error on  $\mu = 5 \log d_L + K$  of  $\sigma_{\mu,stat.} = 0.1$  due to the uncertainty of the corrected apparent magnitudes. We also consider a systematic error given by [63]  $\sigma_{\mu,syst.} = 0.02(1+z)/2.7$ .

For both Supernovae samples, present and forecasted, we marginalize over the absolute magnitude of the sample.

## 4. Results

For the different data sets we compute (or forecast, for future data) the constraints on the first three coefficients of the Chebyshev expansion, assuming a flat  $\Lambda$ CDM with  $H_0 = 73.2 \text{ Km s}^{-1} \text{ Mpc}^{-1}$  and  $\Omega_m = 0.24$  fiducial model with the priors described above and errors on  $H(z)$  and  $d_A(z)$  and  $d_L(z)$  as outlined in §3. For Supernovae and galaxy ages data the analysis is performed exploring the likelihood surface via a Markov Chain Monte Carlo. For the BAO surveys we use both a Markov Chain Monte Carlo and a



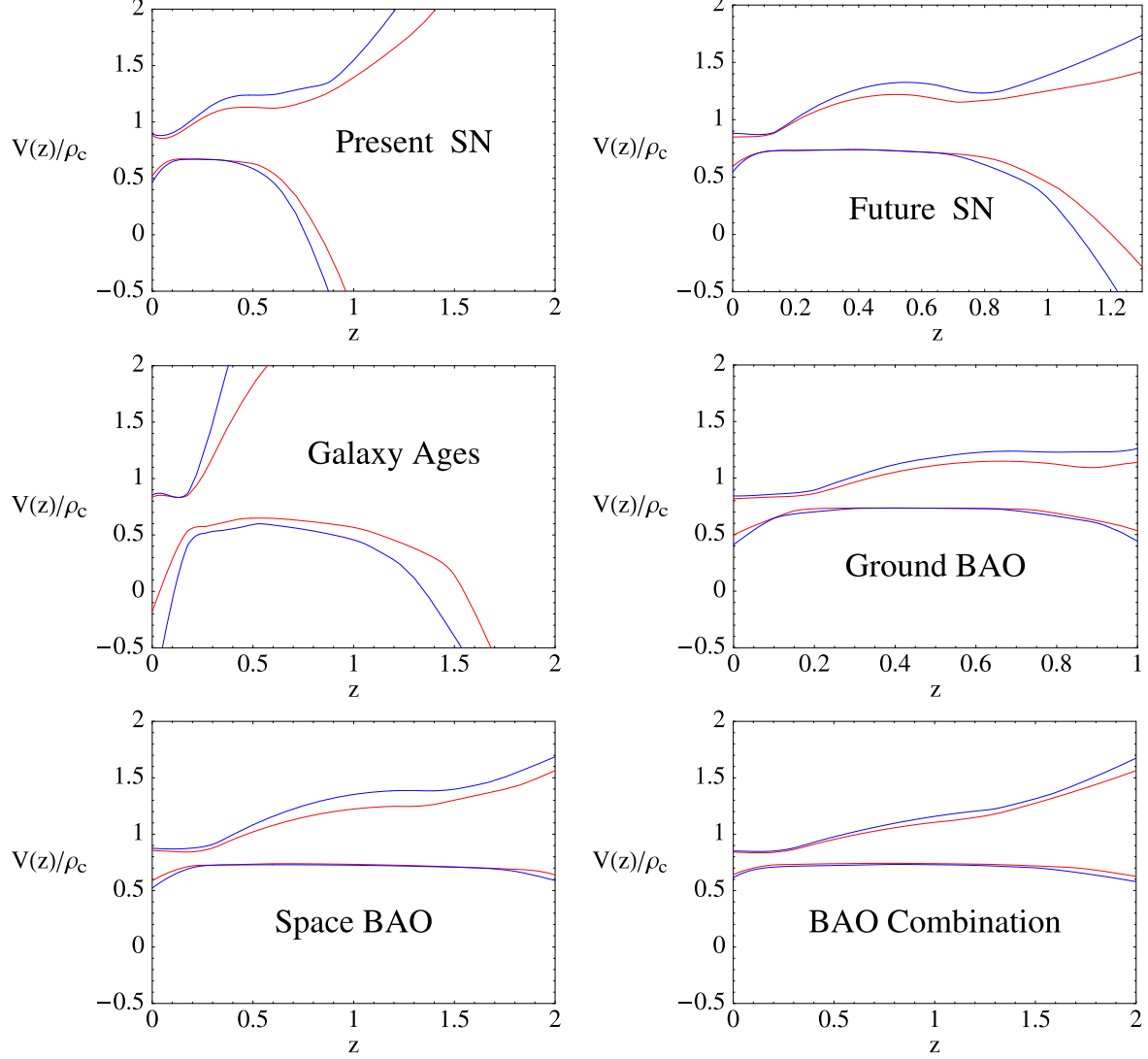


**Figure 1.**  $1$  and  $2\sigma$  constraints on the reconstructed potential as a function of redshift  $V(z)$  from present SN data (top left), SN data from a future-space-based experiment (top right), galaxy ages (middle left), “ground” BAO survey (middle right), “space” BAO survey (bottom left) and the combination of the two BAO surveys (bottom right).

Fisher matrix approach, finding good agreement between the two techniques. Here we present the results of the Fisher matrix analysis.

The constraints on the  $\lambda_i$  thus derived can be translated into constraints on the potential using Eq. (6). In Fig. 1 we show the results of this reconstruction for Supernovae (present and future, top panels) galaxy ages (left middle panel), “ground” BAO survey (middle right), “space” BAO survey (lower left) and the combination of the two BAO surveys (lower right).

Notice that the constraints set by all the datasets considered are strongest between  $z \sim 0.1 - 0.3$ . This is a consequence of the recent dominance of dark energy in the cosmological history and translates in a strong linear degeneracy between  $\lambda_0$  and  $\lambda_1$  as discussed below.

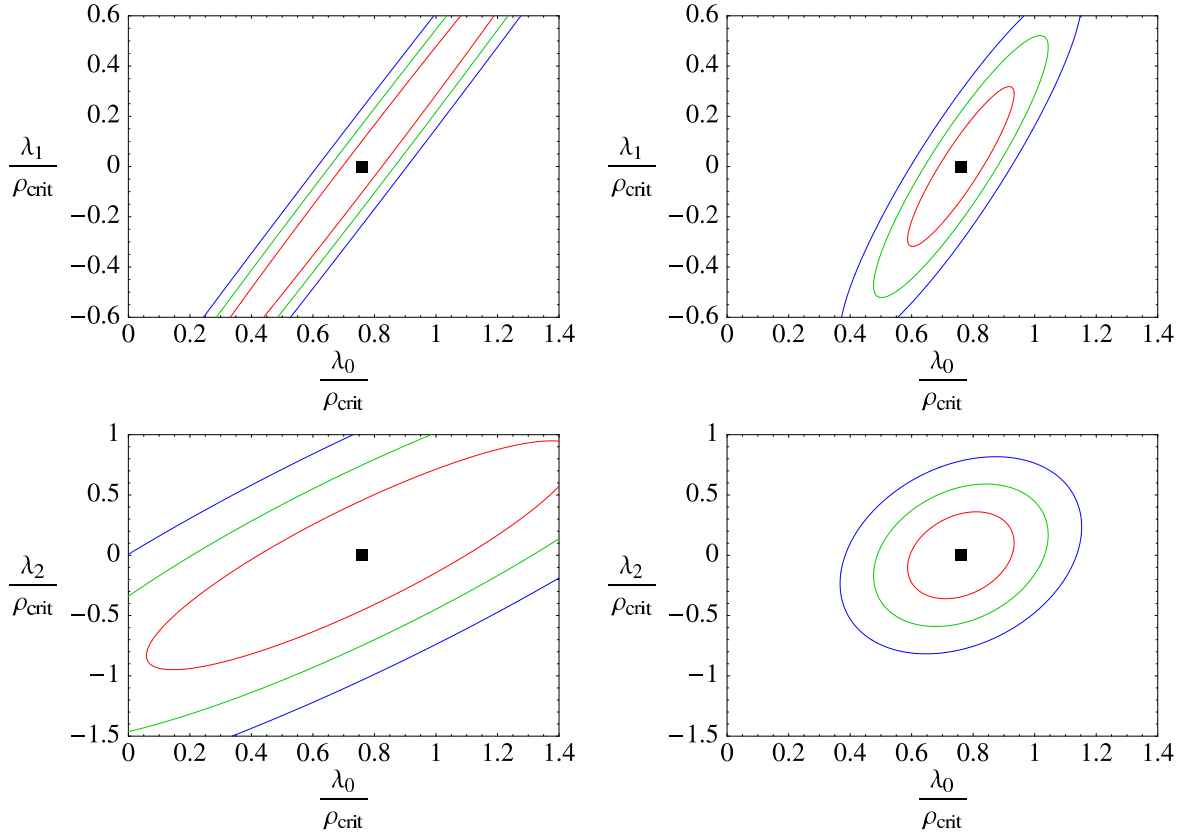


**Figure 2.** 1, 2 and 3  $\sigma$  contours for  $\lambda_0$ ,  $\lambda_1$  (upper panels) and  $\lambda_0$ ,  $\lambda_2$  (lower panels) from measurements of  $d_A(z)$  (left) and  $H(z)$  (right) alone, for a “ground” BAO survey. While the fractional error in  $d_A(z)$  is approximately half of the error in  $H(z)$ , the direct dependence of  $H(z)$  on  $\lambda_i$  coefficients through Eq. (8) yields stronger constraints on these parameters.

#### 4.1. Interpretation of the reconstructed $V(z)$

It can be seen from Eqs. (13) and (14) that the fractional error in  $d_A(z)$  is approximately half of the error in  $H(z)$ . However, there is a direct dependence of  $H(z)$  on  $\lambda_i$  coefficients through Eq. (8), while the relation with  $d_A(z)$  involves an integral and the bounds derived from the information on  $d_A(z)$  are generally weaker than those derived from the measurement of  $H(z)$ . As an example, in Figs. 2 and 3, we show the 1, 2 and 3  $\sigma$  constraints that a “ground” or “space” BAO experiment could respectively place on  $\lambda_0$ ,  $\lambda_1$  and  $\lambda_2$  using only the information on  $d_A(z)$  (left) and on  $H(z)$  (right). Notice that the constraints derived from the information on  $H(z)$  are much tighter. Indeed, we found that, with information on  $d_A(z)$  or  $d_L(z)$  alone, there is a degeneracy between  $\lambda_0$  and  $\lambda_2$ , as shown in the bottom left panel of Figs. 2 and 3 and the right panel of Fig. 4 in Ref. [36]. This degeneracy is lifted by data constraining  $H(z)$  as can be seen in the bottom right panel of Figs. 2 and 3 and the right panel of Figs. 3 and 6 in Ref. [36]. This favors spectroscopic surveys, which can measure  $H(z)$ , over photometric surveys with large photo- $z$  errors which can only measure  $d_A(z)$ .

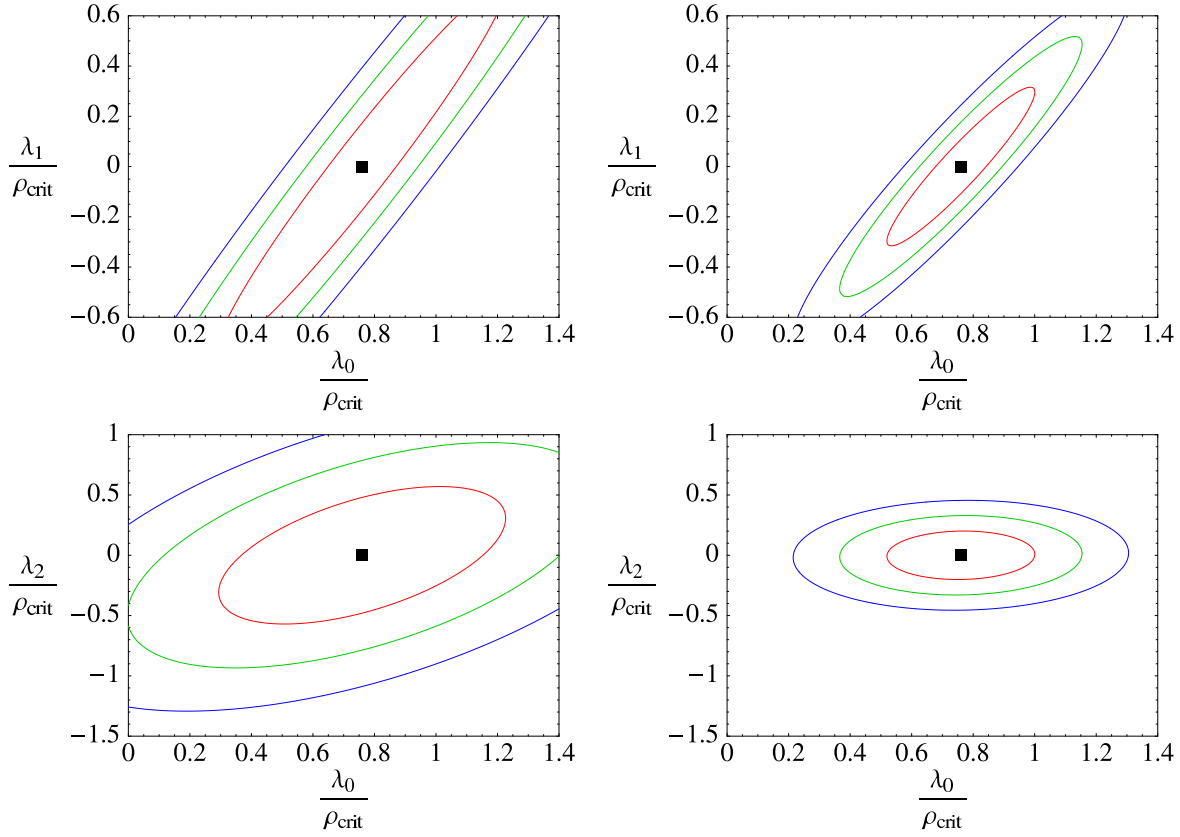


**Figure 3.** 1, 2 and 3  $\sigma$  contours for  $\lambda_0$ ,  $\lambda_1$  and  $\lambda_2$  from measurements of  $d_A(z)$  (left) and  $H(z)$  (right) alone, for a “space” BAO survey. While the fractional error in  $d_A(z)$  is approximately half of the error in  $H(z)$ , the direct dependence of  $H(z)$  on  $\lambda_i$  coefficients through Eq. (8) yields stronger constraints on these parameters.

Let us consider more closely the strong degeneracy between  $\lambda_0$  and  $\lambda_1$  in the top panels of Figs. 2 and 3 and in Figs. 3, 4 and 6 of Ref. [36]. This degeneracy is present in all the datasets we considered but it is more pronounced when no information on  $H(z)$  is available and the sensitivity to the  $\lambda_i$  coefficients relies in integrals like  $d_A(z)$  or  $d_L(z)$  as for Supernovae data. This degeneracy is described by a linear relation between  $\lambda_0$  and  $\lambda_1$  of the form:

$$\lambda_0 = \alpha \lambda_1 + \beta. \quad (18)$$

This implies, to first order in the Chebyshev expansion of Eq. (6):

$$V(z) = (\alpha - 1)\lambda_1 + \beta + \lambda_1 \frac{2z}{z_{max}}. \quad (19)$$

Then, for any value of  $\lambda_1$  along this degeneracy, there is a redshift  $z = z_{max}(1 - \alpha)/2$  for which the value of the potential is fixed to  $V = \beta$ . For all the datasets we found linear degeneracies between  $\lambda_0$  and  $\lambda_1$  with  $\alpha \lesssim 1$  and  $\beta \sim \Omega_\Lambda$ ; this means that for all datasets the potential is better constrained at low redshift, in order to have  $V \sim \Omega_\Lambda$ . This reflects the fact that cosmological data are more sensitive to the dark energy properties for small

$z$ , since at larger redshifts the matter component dominates and the dependence on  $V(z)$  is subdominant. However the exact transition redshift (where  $\Omega_m = \Omega_{DE}$ ) depends on the shape of the dark energy potential.

As for the effect of considering non-flat geometries we find that, with the prior of  $\sigma_k = 0.03$  in  $\Omega_k$  we consider, the effect on the extraction of the DE properties is very small, only slightly increasing the error in the reconstructed parameters. However, loosening the prior on  $\Omega_k$  can severely spoil the constraints shown here significantly worsening the degeneracies among the  $\lambda_i$  coefficients. As an example we show in Fig. 4 the effect on the constraints of the first three  $\lambda_i$  by the “space” BAO survey for different values of the prior on  $\Omega_k$ , 0, 0.03, 0.1 and 1.

Notice that, in spite of the lack of data for  $z < 1$ , the “space”-type survey is placing strong constraints also in that redshift region. This is a consequence of *a)* the priors imposed at  $z = 0$ , *b)* the very accurate data for  $z > 1$  and *c)* the information on  $w(z)$  enclosed in the  $d_A(z)$  constraints, making it possible to interpolate the potential given by our smooth parameterization to the low redshift regime. Therefore, the combination of the two surveys does not provide a significant improvement of the constraints on  $V(z)$  over the “space” survey alone, however these constraints are much more robust since both experiments now cover the whole redshift range shown in Fig. 1.

#### 4.2. Reconstructed $V(\phi)$

Eq. (10) also enables us to reconstruct  $\Delta\phi(z)$  from  $V(z)$  thus constraining  $V(\phi)$ . Fig. 5 shows the results of such a reconstruction for the 68% best models for the different datasets. Note that, upon integration of Eq. (10) up to  $z_{max}$ , a range of  $\Delta\phi(z)$  can be obtained up to a maximum value when  $z = z_{max}$ . This maximum value will strongly depend on the actual model that is integrated and on how strongly the field evolves in that model. Thus, not all values for  $\Delta\phi$  are allowed and showing the 1 and 2  $\sigma$  contours would not be fully correct. Indeed, for the  $\Lambda$ CDM Eq. (10) will always yield  $\Delta\phi(z) = 0$  regardless of  $z_{max}$ . If the constraints placed by a given data set on the model are tightly centered around the  $\Lambda$ CDM very small values of  $\Delta\phi(z)$  will be recovered from such models.

### 5. Reconstruction of the Equation of State

It is widespread to parameterize dark energy not by the scalar field potential but by its equation of state. As long as the equation of state  $w$  is  $> -1$ , parameterizing the dynamics of dark energy through the evolution of its effective equation of state is equivalent to considering the redshift evolution of the dark energy potential. However if we want to allow  $w < -1$  then the scalar field description as presented above fails.

Thus, considering the evolution of an effective equation of state is more general than considering the potential of a scalar field. In this case it is easier to relate  $w(z)$  with the observables. Expanding the redshift dependence of the equation of state in

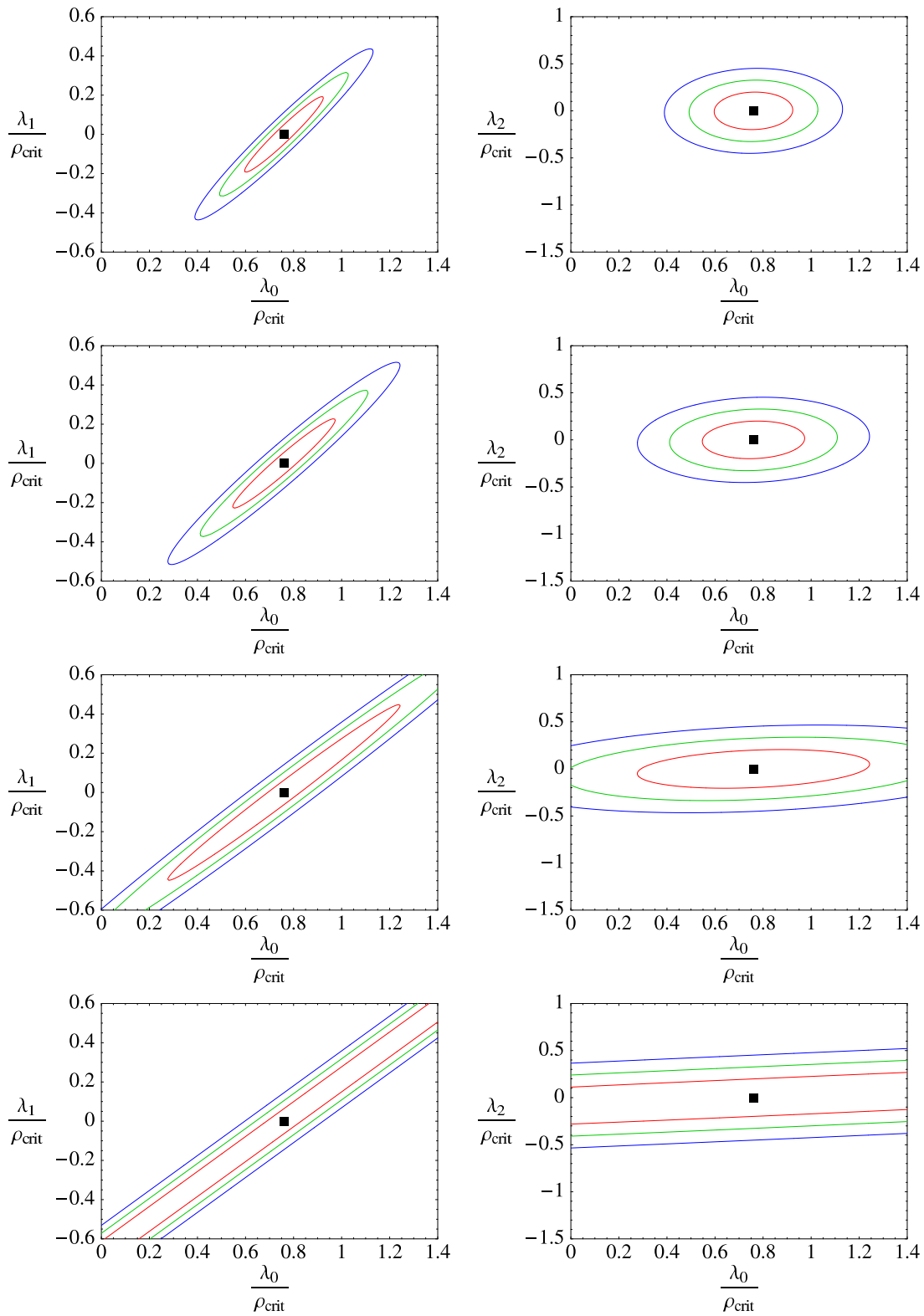


**Figure 4.** 1, 2 and 3  $\sigma$  contours for  $\lambda_0$ ,  $\lambda_1$  and  $\lambda_2$  for a "space" BAO survey for different values of the prior on  $\Omega_k$ , 0, 0.03, 0.1 and 1.

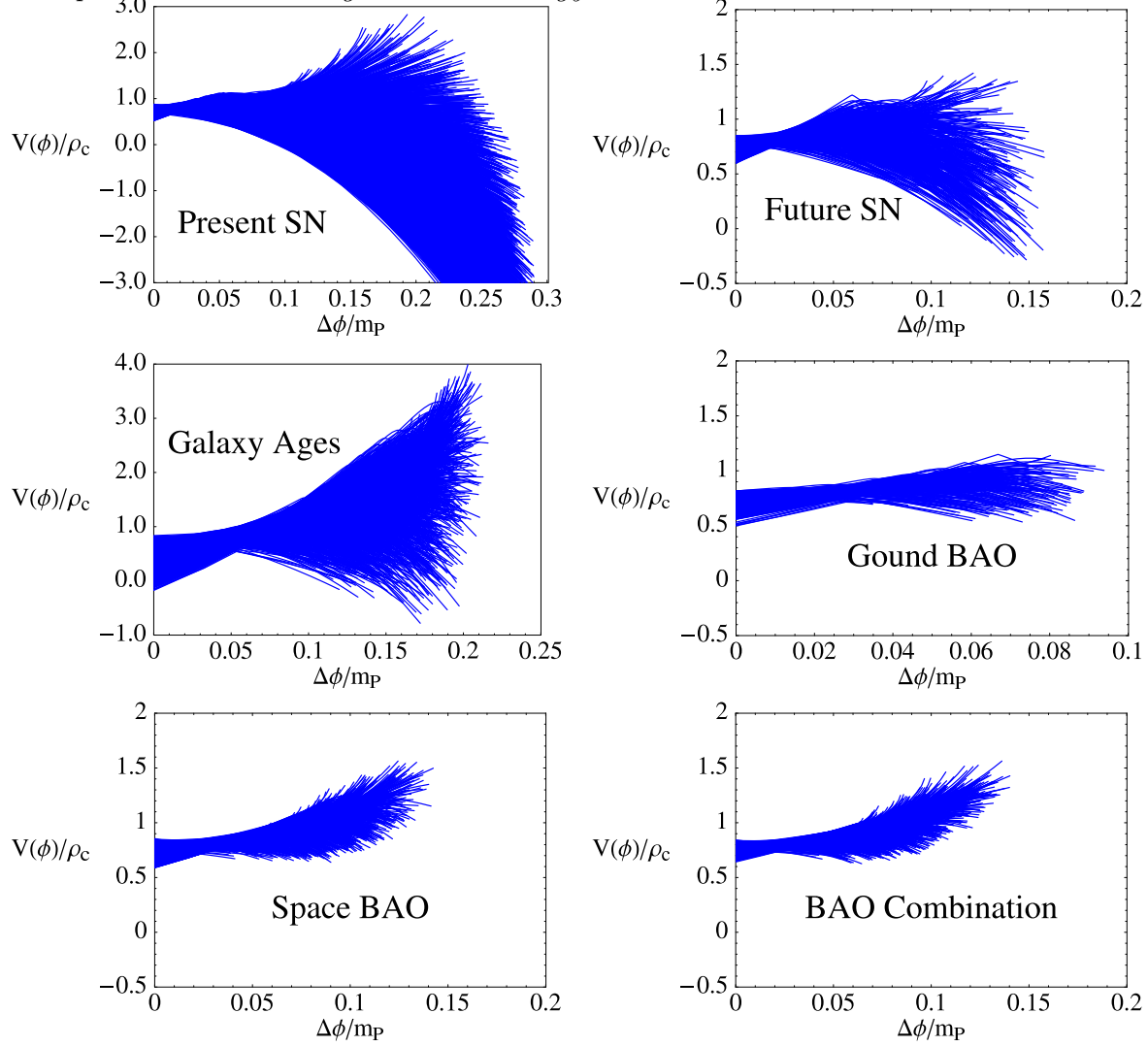


**Figure 5.** Instead of reporting the  $1$  and  $2\sigma$  contours, we plot the reconstructed  $V(\phi)$  for the 68% best models for the different datasets (see text for more details).

Chebyshev polynomials analogously to the expansion of  $V(z)$ :

$$w(z) \simeq \sum_{i=0}^N \omega_i T(x(z)) \quad (20)$$

and substituting in the first Friedmann equation we would have:

$$H^2(\omega_i, z) \simeq H_0^2 \left[ \Omega_{m,0}(1+z)^3 + \Omega_{k,0}(1+z)^2 + (1 - \Omega_{m,0} - \Omega_{k,0})(1+z)^3 \exp \left( \frac{3}{2} z_{max} \sum_{n=0}^N \omega_n G_n(z) \right) \right], \quad (21)$$

where now

$$G_i(z) = \int_{-1}^{2z/z_{max}-1} T_i(x)(a+bx)^{-1} dx. \quad (22)$$

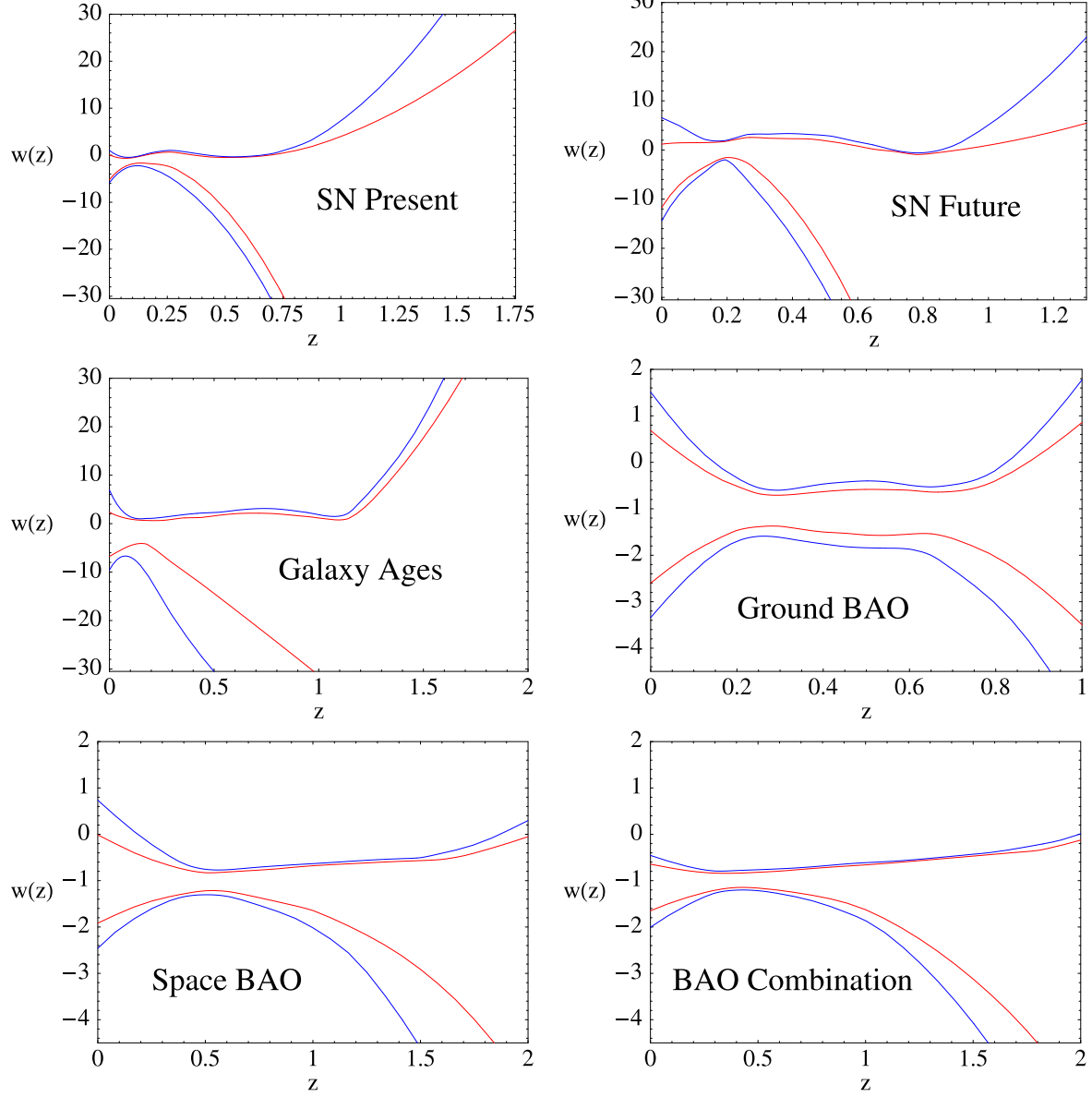


**Figure 6.**  $1$  and  $2\sigma$  constraints on the DE equation of state from present SN data (top left), SN data from a future-space-based experiment (top right), galaxy ages (middle left), “ground” BAO survey (middle right), “space” BAO survey (bottom left) and the combination of the two BAO surveys (bottom right).

Note that in this parameterization the present-day value of  $w$  is given by

$$w_0 = \sum_{i=0}^N (-1)^i \omega_i \quad (23)$$

Eqs. (20–22) are a generalization of sec 3 of [36] to non flat geometries.

We study the constraints that the datasets above can put on the DE equation of state through (21) expanding the dark energy equation state up to second order in Chebyshev polynomials. We perform forecasts using MCMC’s. As in Sec. 4,  $H_0$ ,  $\Omega_m$  and  $\Omega_k$  are parameters which we marginalize over. The same priors quoted before are

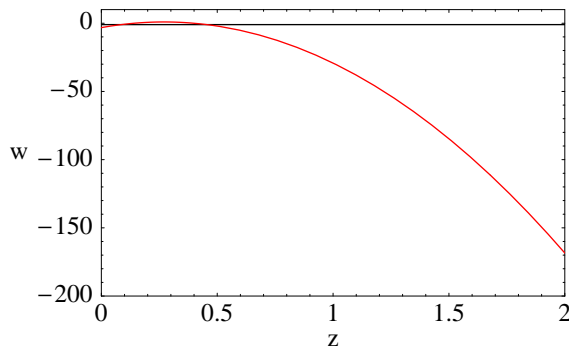


**Figure 7.** Equation of state parameter for a model lying along the degeneracy given by dataset that can only constrain  $d_A$  or  $d_L$ . For comparison also the  $\Lambda$ CDM case is shown ( $w = -1$ ).

also assumed here. We show the results in Fig. 6. As for the reconstruction of  $V(z)$ , dark energy properties are best constrained at  $z \lesssim 0.3$  and the  $H(z)$  determination is crucial in constraining the dark energy evolution especially for non-trivial deviations from a constant equation of state parameter.

Analogously to the case of the reconstruction of  $V(z)$ , since the dependence of  $H(z)$  on  $w(z)$  is through an integral, for quantities that depend on integrals of  $1/H(z)$  such as  $d_A(z)$  or  $d_L(z)$ , the information on  $w(z)$  is even more diluted. This explains the weak constraints found in Fig. 6 for all the datasets except the two BAO surveys. The deterioration of the bounds comes mainly through a degeneracy between  $w_0$  and  $w_1$  that can span down to  $w_0 \sim -100$  and  $w_1 \sim -100$  if only information on  $d_A$  or  $d_L$  is available. This degeneracy is solved with information on  $H(z)$ . As an example let us consider a model lying within this degeneracy. The parameters for this model are:  $H_0 = 70.38$  km/s/Mpc,  $\Omega_m = 0.28$ ,  $\Omega_k = 0.025$ ,  $w_0 = -57.51$ ,  $w_1 = -82.63$ ,  $w_2 = -28.31$  and its equation of state parameter is shown in Fig. 7 along with the  $\Lambda$ CDM values  $w = -1$  for comparison. From Eq. (23), we can see that these parameters will still give  $w = -3.19$  today, however for  $z = 2$ ,  $w = -168$ .

In Fig. 8 we show the comparison between  $H(z)$  and  $d_A(z)$  for this model and for the  $\Lambda$ CDM model. From the figure it is clear that information on  $d_A(z)$  alone does not suffice to discriminate between the two, while the differences in  $H(z)$  between the two models are large. Even with these extreme values of the parameters, this model mimics the  $d_A(z)$  behaviour of the  $\Lambda$ CDM, but has a significantly different  $H(z)$  which oscillates around the  $\Lambda$ CDM  $H(z)$ . Thus, upon integrating  $H(z)$  to obtain  $d_A(z)$ , the regions where the model is above the  $\Lambda$ CDM compensate the ones where it is below. A measurement of  $H(z)$ , however, can easily distinguish the two models. We were not able to reproduce this behaviour to the same degree with a two-parameter description of the dark energy equation of state dynamics. This example highlights an important open issue in dark energy studies: constraints on dark energy parameters coming from



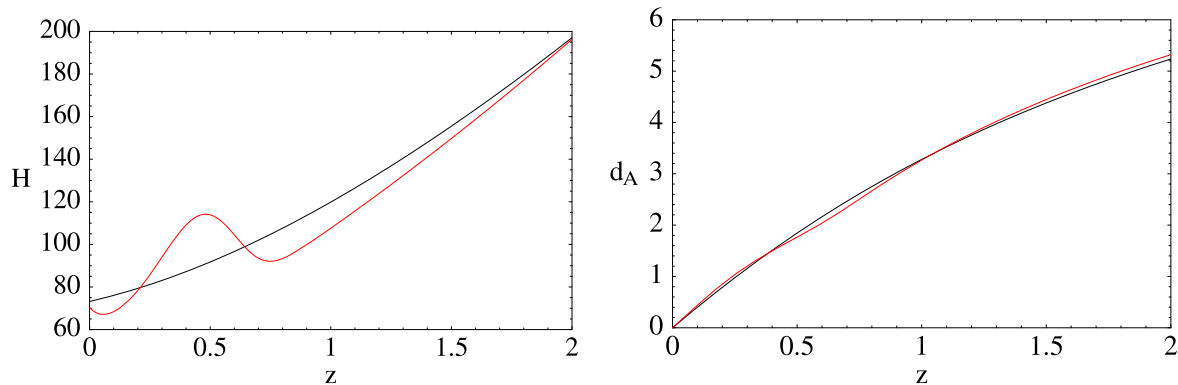


**Figure 8.** Comparison of  $H(z)$  and  $d_A(z)$  for the example model described in the text and in Fig. 7 and for the  $\Lambda$ CDM model.

measurement of integrated quantities depend crucially on the choice of the dark energy parameterization [64]: in the absence of a theoretical motivation for a parameterization of dark energy properties, forecasts and constraints become crucially model-dependent.

We have checked that fixing  $\omega_2 = 0$  and  $\Omega_k = 0$ , with just a two parameter description of the dynamics of the dark energy equation of state via  $\omega_0$  and  $\omega_1$ , we are able to recover similar constraints to those found with alternative descriptions with two parameters. Note that the linear parameterization in [34, 65], corresponds to  $\omega_i = 0$  for  $i > 1$ , and in particular  $w_0 = \omega_0 - \omega_1$  and  $w' = 2\omega_1/z_{max}$ . Finally the linear parameterization in a [66, 67],  $w = w_0 + w_a z/(1+z)$  for  $|w_a| \ll w_0$  can be closely approximated by  $\omega_i = 0$  for  $i > 2$ , with the constraint (20). Ref. [68] pointed out that a simple, 2-parameter fit may introduce biases: the expansion (42) allows one to include more parameters by increasing  $N$  as the observational data improve.

The analysis shown here shows that, increasing the number of parameters seriously spoils our ability to constrain  $w(z)$  except at small redshifts. As for the constraints on the potential, the stronger constraints at low redshifts are related to very pronounced degeneracies between  $w_0$  and  $w_1$ . This degeneracies are much less important for the two BAO surveys, but the rest of the datasets considered can only effectively constrain the dark energy equation of state at small values of  $z$ . For a constant equation of state ( $\omega_i = 0$  for  $i > 0$ ) the bound derived will roughly correspond to the narrowest allowed region at small redshifts.

## 6. Conclusions

We have generalized to non-flat geometries the formalism of [36] to reconstruct the dark energy potential. This approach makes use of quantities similar to the horizon flow parameters used to reconstruct the inflation potential [39, 40]. The method can, in principle, be made non-parametric, but present and forthcoming data do not allow a fully non-parametric reconstruction. We have therefore considered a parametric description in term of Chebyshev polynomials which, for all our applications, we have truncated to

second order. For completeness we have also considered a reconstruction of the dark energy equation of state redshift dependence in terms of Chebyshev polynomials, also generalizing to non-flat geometries the results of [36].

We have considered present measurements of  $H(z)$  from ages of passively evolving galaxies [50, 36], future Baryon Acoustic Oscillation (BAO) surveys and present and future type IA supernova surveys and investigated their constraints on dark energy properties.

We present present and forecast constraints both on  $V(z)$  (Fig. 1) and, more interestingly, on  $V(\phi)$  (Fig. 5), in sec. 4. Model building for dark energy which rely on simple single-field models and provide physically motivated potentials should satisfy the constraints shown in the left top and middle panels of Fig. 5. In the future, the expected constraints can be as tight as those shown in the two bottom panels of Fig 5. More complicated models (multi fields etc.) should produce a redshift evolution of the effective dark energy potential which satisfies the constraints in the left top and middle panel of Fig. 1. The expected future constraints can be as tight as shown in the bottom panels of Fig. 1.

We find that relaxing the flatness assumption increases slightly the errors on the reconstructed dark energy evolution, but does not generate significant degeneracies, provided that a modest prior on geometry is imposed  $\sigma_k = 0.03$  (e.g., Fig. 4).

Dark energy properties are best constrained at  $z \lesssim 0.3$ : this is the result of the late-time dominance of dark energy. Under the assumptions made here, the most crucial being the assumption of a smooth  $V(z)$  or  $w(z)$ , we find that high redshift ( $z < 2$ ) measurements of both  $H(z)$  and  $d_A$  are more powerful than low  $z$  measurements.

When constraining the redshift evolution of both the dark energy potential  $V(z)$  or the dark energy equation of state parameter  $w(z)$  with measurements of integrated quantities such as  $d_A$  or  $d_L$ , there are large degeneracies among the parameters. These degeneracies are greatly reduced or removed with measurements of  $H(z)$ , such as those provided e.g., by future BAO surveys. This is illustrated in Figs. 2 and 3 for the potential reconstruction. While the  $H(z)$  constraint is generally weaker than the  $d_A(z)$  constraints,  $H(z)$  is more directly related to the dark energy properties and thus offers more powerful dark energy constraints. We have illustrated this with an example of a model which lays on the “ $d_A$ -degeneracy” for the reconstruction of  $w(z)$ . This model produces  $d_A(z)$  and  $d_L(z)$  virtually indistinguishable from that of the  $\Lambda$ CDM, however the  $H(z)$  are different and easily distinguishable from BAO measurements with  $H(z)$  information.

This highlights an important open issue in dark energy studies: constraints on dark energy parameters coming from measurement of integrated quantities such as  $d_A$  or  $d_L$  depend crucially on the choice of the dark energy parameterization [e.g., [64]]: in the absence of a theoretical motivation for a parameterization of dark energy properties, forecasts and constraints become crucially model-dependent. The dependence of the constraints on the assumed dark energy parameterization becomes evident only when considering non-trivial deviations from a  $\Lambda$ CDM model (e.g., deviations from a constant

$w$  or generic shape of the potential). This issue is greatly alleviated by measurements that carry information on  $H(z)$ .

## Acknowledgments

EFM acknowledges financial support from the Max Planck Institut für Physik. LV acknowledges support of FP7-PEOPLE-2007-4-3-IRGn202182 and CSIC I3 grant 200750I034. This work was supported in part by the Spanish Ministry of Education and Science (MEC) through the Consolider Ingenio-2010 program, under project CSD2007-00060 Physics of the Accelerating Universe (PAU).

## References

- [1] D. N. Spergel, L. Verde, H. V. Peiris, E. Komatsu, M. R. Nolta, C. L. Bennett, M. Halpern, G. Hinshaw, N. Jarosik, A. Kogut, M. Limon, S. S. Meyer, L. Page, G. S. Tucker, J. L. Weiland, E. Wollack, and E. L. Wright, *First-Year Wilkinson Microwave Anisotropy Probe (WMAP) Observations: Determination of Cosmological Parameters*, *ApJS* **148** (Sept., 2003) 175–194.
- [2] Spergel, R. Bean, O. Doré, M. R. Nolta, C. L. Bennett, J. Dunkley, G. Hinshaw, N. Jarosik, E. Komatsu, L. Page, H. V. Peiris, L. Verde, M. Halpern, R. S. Hill, A. Kogut, M. Limon, S. S. Meyer, N. Odegard, G. S. Tucker, J. L. Weiland, E. Wollack, and E. L. Wright, *Three-Year Wilkinson Microwave Anisotropy Probe (WMAP) Observations: Implications for Cosmology*, *ApJS* **170** (June, 2007) 377–408, [[arXiv:astro-ph/0603449](#)].
- [3] J. Dunkley, E. Komatsu, M. R. Nolta, D. N. Spergel, D. Larson, G. Hinshaw, L. Page, C. L. Bennett, B. Gold, N. Jarosik, J. L. Weiland, M. Halpern, R. S. Hill, A. Kogut, M. Limon, S. S. Meyer, G. S. Tucker, E. Wollack, and E. L. Wright, *Five-Year Wilkinson Microwave Anisotropy Probe (WMAP) Observations: Likelihoods and Parameters from the WMAP data*, *ArXiv e-prints* **803** (Mar., 2008) [[0803.0586](#)].
- [4] E. Komatsu, J. Dunkley, M. R. Nolta, C. L. Bennett, B. Gold, G. Hinshaw, N. Jarosik, D. Larson, M. Limon, L. Page, D. N. Spergel, M. Halpern, R. S. Hill, A. Kogut, S. S. Meyer, G. S. Tucker, J. L. Weiland, E. Wollack, and E. L. Wright, *Five-Year Wilkinson Microwave Anisotropy Probe (WMAP) Observations: Cosmological Interpretation*, *ArXiv e-prints* **803** (Mar., 2008) [[0803.0547](#)].
- [5] W. M. Wood-Vasey, G. Miknaitis, C. W. Stubbs, S. Jha, A. G. Riess, P. M. Garnavich, R. P. Kirshner, C. Aguilera, A. C. Becker, J. W. Blackman, S. Blondin, P. Challis, A. Clocchiatti, A. Conley, R. Covarrubias, T. M. Davis, A. V. Filippenko, R. J. Foley, A. Garg, M. Hicken, K. Krisciunas, B. Leibundgut, W. Li, T. Matheson, A. Miceli, G. Narayan, G. Pignata, J. L. Prieto, A. Rest, M. E. Salvo, B. P. Schmidt, R. C. Smith, J. Sollerman, J. Spyromilio, J. L. Tonry, N. B. Suntzeff, and A. Zenteno, *Observational Constraints on the Nature of Dark Energy: First Cosmological Results from the ESSENCE Supernova Survey*, *ApJ* **666** (Sept., 2007) 694–715, [[arXiv:astro-ph/0701041](#)].
- [6] SDSS Collaboration, M. Tegmark *et. al.*, *Cosmological Constraints from the SDSS Luminous Red Galaxies*, *Phys. Rev.* **D74** (2006) 123507, [[astro-ph/0608632](#)].
- [7] W. J. Percival, R. C. Nichol, D. J. Eisenstein, J. A. Frieman, M. Fukugita, J. Loveday, A. C. Pope, D. P. Schneider, A. S. Szalay, M. Tegmark, M. S. Vogeley, D. H. Weinberg, I. Zehavi, N. A. Bahcall, J. Brinkmann, A. J. Connolly, and A. Meiksin, *The Shape of the Sloan Digital Sky Survey Data Release 5 Galaxy Power Spectrum*, *ApJ* **657** (Mar., 2007) 645–663, [[arXiv:astro-ph/0608636](#)].

- [8] R. R. Caldwell, R. Dave, and P. J. Steinhardt, *Quintessential Cosmology Novel Models of Cosmological Structure Formation*, *ApJSS* **261** (1998) 303–310.
- [9] I. Zlatev, L. Wang, and P. J. Steinhardt, *Quintessence, Cosmic Coincidence, and the Cosmological Constant*, *Physical Review Letters* **82** (Feb., 1999) 896–899, [[arXiv:astro-ph/9807002](#)].
- [10] L. Wang, R. R. Caldwell, J. P. Ostriker, and P. J. Steinhardt, *Cosmic Concordance and Quintessence*, *ApJ* **530** (Feb., 2000) 17–35, [[arXiv:astro-ph/9901388](#)].
- [11] P. J. E. Peebles and B. Ratra, *Cosmology with a time-variable cosmological 'constant'*, *ApJL* **325** (Feb., 1988) L17–L20.
- [12] B. Ratra and P. J. E. Peebles, *Cosmological consequences of a rolling homogeneous scalar field*, *Phys. Rev. D* **37** (June, 1988) 3406–3427.
- [13] B. Ratra and P. J. E. Peebles *Phys. Rev. D* **52** (1995) 1837.
- [14] C. Wetterich, *An asymptotically vanishing time-dependent cosmological "constant"*, *A* **301** (Sept., 1995) 321–+, [[arXiv:hep-th/9408025](#)].
- [15] P. J. Steinhardt, *A quintessential introduction to dark energy*, *Royal Society of London Philosophical Transactions Series A* **361** (Nov., 2003) 2497–2513.
- [16] G. Dvali, G. Gabadadze, and M. Porrati, *4D gravity on a brane in 5D Minkowski space*, *Physics Letters B* **485** (July, 2000) 208–214.
- [17] C. Deffayet, G. Dvali, and G. Gabadadze, *Accelerated universe from gravity leaking to extra dimensions*, *PRD* **65** (Feb., 2002) 044023–+.
- [18] S. M. Carroll, V. Duvvuri, M. Trodden, and M. S. Turner, *Is cosmic speed-up due to new gravitational physics?*, *Phys. Rev. D* **70** (2004) 043528, [[astro-ph/0306438](#)].
- [19] S. M. Carroll, A. de Felice, V. Duvvuri, D. A. Easson, M. Trodden, and M. S. Turner, *Cosmology of generalized modified gravity models*, *Phys. Rev. D* **71** (Mar., 2005) 063513–+, [[arXiv:astro-ph/0410031](#)].
- [20] S. Capozziello, V. F. Cardone, and A. Troisi, *Reconciling dark energy models with  $f(R)$  theories*, *Phys. Rev. D* **71** (Feb., 2005) 043503–+, [[arXiv:astro-ph/0501426](#)].
- [21] S. Nojiri and S. D. Odintsov, *Modified Gravity with  $\ln R$  Terms and Cosmic Acceleration*, *General Relativity and Gravitation* **36** (Aug., 2004) 1765–1780, [[arXiv:hep-th/0308176](#)].
- [22] A. D. Dolgov and M. Kawasaki, *Can modified gravity explain accelerated cosmic expansion?*, *Physics Letters B* **573** (Oct., 2003) 1–4, [[arXiv:astro-ph/0307285](#)].
- [23] W. Hu and I. Sawicki, *Parametrized post-Friedmann framework for modified gravity*, *Phys. Rev. D* **76** (Nov., 2007) 104043–+, [[arXiv:0708.1190](#)].
- [24] V. Acquaviva, C. Baccigalupi, S. M. Leach, A. R. Liddle, and F. Perrotta, *Structure formation constraints on the Jordan-Brans-Dicke theory*, *Phys. Rev. D* **71** (May, 2005) 104025–+, [[arXiv:astro-ph/0412052](#)].
- [25] V. Acquaviva and L. Verde, *Observational signatures of Jordan Brans Dicke theories of gravity*, *Journal of Cosmology and Astro-Particle Physics* **12** (Dec., 2007) 1–+, [[arXiv:0709.0082](#)].
- [26] K. Enqvist, *Lemaitre Tolman Bondi model and accelerating expansion*, *General Relativity and Gravitation* **40** (Feb., 2008) 451–466, [[arXiv:0709.2044](#)].
- [27] S. Räsänen, *Accelerated expansion from structure formation*, *Journal of Cosmology and Astro-Particle Physics* **11** (Nov., 2006) 3–+, [[arXiv:astro-ph/0607626](#)].
- [28] T. Kai, H. Kozaki, K. Nakao, Y. Nambu, and C. Yoo, *Can Inhomogeneities Accelerate the Cosmic Volume Expansion?*, *Progress of Theoretical Physics* **117** (Feb., 2007) 229–240, [[arXiv:gr-qc/0605120](#)].
- [29] E. W. Kolb, S. Matarrese, and A. Riotto, *On cosmic acceleration without dark energy*, *New Journal of Physics* **8** (Dec., 2006) 322–+, [[arXiv:astro-ph/0506534](#)].
- [30] I. Maor, R. Brustein, J. McMahon, and P. J. Steinhardt, *Measuring the equation of state of the universe: Pitfalls and prospects*, *Phys. Rev. D* **65** (June, 2002) 123003–+, [[arXiv:astro-ph/0112526](#)].
- [31] D. J. Eisenstein and W. Hu, *Baryonic Features in the Matter Transfer Function*, *ApJ* **496** (Mar.,

- 1998) 605–+, [[arXiv:astro-ph/9709112](#)].
- [32] D. J. Eisenstein, I. Zehavi, D. W. Hogg, R. Scoccimarro, M. R. Blanton, R. C. Nichol, R. Scranton, H.-J. Seo, M. Tegmark, Z. Zheng, S. F. Anderson, J. Annis, N. Bahcall, J. Brinkmann, S. Burles, F. J. Castander, A. Connolly, I. Csabai, M. Doi, M. Fukugita, J. A. Frieman, K. Glazebrook, J. E. Gunn, J. S. Hendry, G. Hennessy, Z. Ivezić, S. Kent, G. R. Knapp, H. Lin, Y.-S. Loh, R. H. Lupton, B. Margon, T. A. McKay, A. Meiksin, J. A. Munn, A. Pope, M. W. Richmond, D. Schlegel, D. P. Schneider, K. Shimasaku, C. Stoughton, M. A. Strauss, M. SubbaRao, A. S. Szalay, I. Szapudi, D. L. Tucker, B. Yanny, and D. G. York, *Detection of the Baryon Acoustic Peak in the Large-Scale Correlation Function of SDSS Luminous Red Galaxies*, *ApJ* **633** (Nov., 2005) 560–574, [[arXiv:astro-ph/0501171](#)].
  - [33] S. Cole, C. M. Baugh, J. Bland-Hawthorn, T. Bridges, R. Cannon, S. Cole, M. Colless, C. Collins, W. Couch, G. Dalton, R. De Propris, S. P. Driver, G. Efstathiou, R. S. Ellis, C. S. Frenk, and et al., *The 2dF Galaxy Redshift Survey: power-spectrum analysis of the final data set and cosmological implications*, *MNRAS* **362** (Sept., 2005) 505–534, [[arXiv:astro-ph/0501174](#)].
  - [34] D. Huterer and M. S. Turner, *Probing the dark energy: Methods and strategies*, *Phys. Rev. D* **64** (2001) 123527, [[astro-ph/0012510](#)].
  - [35] D. Huterer and G. Starkman, *Parameterization of dark-energy properties: A principal-component approach*, *Phys. Rev. Lett.* **90** (2003) 031301 [[arXiv:astro-ph/0207517](#)].
  - [36] J. Simon, L. Verde, and R. Jimenez, *Constraints on the redshift dependence of the dark energy potential*, *Phys. Rev. D* **71** (June, 2005) 123001–+, [[arXiv:astro-ph/0412269](#)].
  - [37] D. Huterer and H. V. Peiris, *Dynamical behavior of generic quintessence potentials: Constraints on key dark energy observables*, *Phys. Rev. D* **75** (2007) 083503 [[arXiv:astro-ph/0610427](#)].
  - [38] C. Clarkson, M. Cortès, and B. Bassett, *Dynamical dark energy or simply cosmic curvature?*, *Journal of Cosmology and Astro-Particle Physics* **8** (Aug., 2007) 11–+, [[arXiv:astro-ph/0702670](#)].
  - [39] D. J. Schwarz, C. A. Terrero-Escalante, and A. A. García, *Higher order corrections to primordial spectra from cosmological inflation*, *Physics Letters B* **517** (Oct., 2001) 243–249, [[arXiv:astro-ph/0106020](#)].
  - [40] S. M. Leach, A. R. Liddle, J. Martin, and D. J. Schwarz, *Cosmological parameter estimation and the inflationary cosmology*, *Phys. Rev. D* **66** (July, 2002) 023515–+, [[arXiv:astro-ph/0202094](#)].
  - [41] P. J. Green and B. W. Silverman, *Nonparametric Regression and Generalized Linear Models*. Chapman and Hall, 1994.
  - [42] C. Sealfon, L. Verde, and R. Jimenez, *Smoothing spline primordial power spectrum reconstruction*, *PRD* **72** (Nov., 2005) 103520–+, [[arXiv:astro-ph/0506707](#)].
  - [43] L. Verde and H. V. Peiris, *On Minimally-Parametric Primordial Power Spectrum Reconstruction and the Evidence for a Red Tilt*, 0802.1219.
  - [44] W. L. Freedman, B. F. Madore, B. K. Gibson, L. Ferrarese, D. D. Kelson, S. Sakai, J. R. Mould, R. C. Kennicutt, H. C. Ford, J. A. Graham, J. P. Huchra, S. M. G. Hughes, G. D. Illingworth, L. M. Macri, and P. B. Stetson, *Final Results from the Hubble Space Telescope Key Project to Measure the Hubble Constant*, *ApJ* **553** (May, 2001) 47–72.
  - [45] <http://www.rssd.esa.int/index.php?project=planck>.
  - [46] Riess A.G. et al. *in preparation* (2008).
  - [47] C. Blake, D. Parkinson, B. Bassett, K. Glazebrook, M. Kunz, and R. C. Nichol, *Universal fitting formulae for baryon oscillation surveys*, *MNRAS* **365** (Jan., 2006) 255–264, [[arXiv:astro-ph/0510239](#)].
  - [48] H.-J. Seo and D. J. Eisenstein, *Probing Dark Energy with Baryonic Acoustic Oscillations from Future Large Galaxy Redshift Surveys*, *ApJ* **598** (Dec., 2003) 720–740, [[arXiv:astro-ph/0307460](#)].
  - [49] C. Blake and S. Bridle, *Cosmology with photometric redshift surveys*, *MNRAS* **363** (Nov., 2005) 1329–1348, [[arXiv:astro-ph/0411713](#)].

- [50] R. Jimenez, L. Verde, T. Treu, and D. Stern, *Constraints on the Equation of State of Dark Energy and the Hubble Constant from Stellar Ages and the Cosmic Microwave Background*, *ApJ* **593** (Aug., 2003) 622–629, [arXiv:astro-ph/0302560].
- [51] D. Stern *et al.* in preparation.
- [52] <http://www.ice.csic.es/personal/verde/clocks.html>.
- [53] T. Treu *et al.*, *The Assembly History of Field Spheroidals: Evolution of Mass-to-light Ratios and Signatures of Recent Star Formation*, *Astrophys. J.* **633**, 174 (2005) [arXiv:astro-ph/0503164].
- [54] R. J. Cool *et al.*, *Luminosity Function Constraints on the Evolution of Massive Red Galaxies Since  $z = 0.9$*  arXiv:0804.4516 [astro-ph].
- [55] A. Heavens, B. Panter, R. Jimenez and J. Dunlop, *The Complete Star Formation History of the Universe*, *Nature* **428** (2004) 625 [arXiv:astro-ph/0403293].
- [56] J. Dunlop, J. Peacock, H. Spinrad, A. Dey, R. Jimenez, D. Stern, and R. Windhorst, *A 3.5-Gyr-old galaxy at redshift 1.55*, *Nature* **381** (June, 1996) 581–584.
- [57] H. Spinrad, A. Dey, D. Stern, J. Dunlop, J. Peacock, R. Jimenez, and R. Windhorst, *LBDS 53W091: an Old, Red Galaxy at  $z=1.552$* , *ApJ* **484** (July, 1997) 581–+, [arXiv:astro-ph/9702233].
- [58] D. Stern, M. Kamionkowski, R. Jimenez, L. Verde, and C. D’Andrea *in preparation* (2008).
- [59] **Supernova Search Team** Collaboration, A. G. Riess *et. al.*, *Observational Evidence from Supernovae for an Accelerating Universe and a Cosmological Constant*, *Astron. J.* **116** (1998) 1009–1038, [astro-ph/9805201].
- [60] **Supernova Cosmology Project** Collaboration, S. Perlmutter *et. al.*, *Measurements of Omega and Lambda from 42 High-Redshift Supernovae*, *Astrophys. J.* **517** (1999) 565–586, [astro-ph/9812133].
- [61] T. M. Davis *et. al.*, *Scrutinizing exotic cosmological models using ESSENCE supernova data combined with other cosmological probes*, *Astrophys. J.* **666** (2007) 716, [astro-ph/0701510].
- [62] A. Albrecht *et. al.*, *Report of the Dark Energy Task Force*, astro-ph/0609591.
- [63] E. V. Linder and D. Huterer, *Importance of Supernovae at  $z \gtrsim 1.5$  to Probe Dark Energy*, *Phys. Rev.* **D67** (2003) 081303, [astro-ph/0208138].
- [64] I. Maor, R. Brustein, and P. J. Steinhardt, *Limitations in Using Luminosity Distance to Determine the Equation of State of the Universe*, *Physical Review Letters* **86** (Jan., 2001) 6–9, [arXiv:astro-ph/0007297].
- [65] J. Weller and A. Albrecht, *Future Supernovae observations as a probe of dark energy*, *Phys. Rev.* **D65** (2002) 103512, [astro-ph/0106079].
- [66] D. P. M. Chevallier and A. Starobinsky *International Journal of Modern Physics D* **10** (2001) 213.
- [67] E. V. Linder, *Exploring the expansion history of the universe*, *Phys. Rev. Lett.* **90** (2003) 091301, [astro-ph/0208512].
- [68] B. A. Bassett, P. S. Corasaniti, and M. Kunz, *The essence of quintessence and the cost of compression*, *Astrophys. J.* **617** (2004) L1–L4, [astro-ph/0407364].